GluCEST in the olfactory cortex as a marker of heightened clinical risk for schizophrenia

Ravi Prakash Reddy Nanga[1], David R. Roalf[2], Hari Hariharan[1], Mark A. Elliott[1], Karthik Prabhakaran[2], Megan Quarmley[2], Paul J. Moberg[2], Ravinder Reddy[1], and Bruce I. Turetsky[2]

[1]*Radiology, University of Pennsylvania Health Systems, Philadelphia, Pennsylvania, United States,* [2]*Psychiatry, University of Pennsylvania, Philadelphia, Pennsylvania, United States*

Introduction: Deficits in olfactory function are a hallmark of schizophrenia. These deficits are reliably observed in multiple olfactory domains, including odor detection threshold (1), identification and hedonic perception (2). Olfactory deficits precede the onset of illness, distinguish adolescents who are developing prodromal symptoms from healthy youths, (3) and *may predict* which vulnerable youths go on to develop schizophrenia (4). Importantly, these behavioral deficits denote fundamental neuroanatomic and neurophysiologic abnormalities that are specific to the peripheral olfactory system and primary olfactory cortex (1). Given the clinical evidence implicating abnormal neurodevelopment in the pathogenesis of schizophrenia, and the potential utility of olfactory measures to predict illness vulnerability, the olfactory system holds distinct promise for understanding neurodevelopmental contributions to schizophrenia pathophysiology. The sensitivity of the olfactory system as a vulnerability marker may be related to its developmental time course, which occurs in close coordination, embryologically, with early forebrain development during the first trimester of pregnancy (5). Adolescence is a critical developmental risk period, during which developmental anomalies or stressors can greatly increase the subsequent risk of schizophrenia (5). As such, early intervention requires valid and reliable methods of identifying youths at highest risk for developing psychosis. Here, we extend this previous work to an investigation of glutamate within the olfactory system in youths at heightened clinical risk for psychosis. We believe that, a hyperglutamatergic state within the olfactory system may be associated with behavioral manifestations and will likely aid in identifying individuals at risk for schizophrenia. Thus, the use of 7.0T GluCEST to map glutamate may yield improved quantification of brain neurochemistry in subjects at risk for schizophrenia.

Methods: All of the human studies were conducted under an approved Institutional Review Board protocol of the University of Pennsylvania. GluCEST MRI was acquired on 7.0T Siemens scanner with a 32-channel phased-array head coil from 16 healthy controls (HC) and 12 individuals at clinical risk for developing schizophrenia (CR). We implemented an optimized within-subject acquisition and analysis pipeline (Figure 1). Upon completion of 3T MRI scanning, each subject's whole-head structural image was analyzed using FreeSurfer (v5.0). The resulting standardized regions of interest (e.g. olfactory cortex, medial orbitofrontal cortex) were extracted and prepared for use at 7.0T. ROIs were then used to prescribe the slice location during 7.0T for GluCEST acquisition. This was accomplished in real-time using the Imscribe tool which was designed to allow reproducible selection of the same anatomical field-of-view in Siemens MRI studies either between subjects or within the same subject over multiple MRI scans (6). The GluCEST imaging parameters were: slice thickness = 5 mm, field of view read = 220 mm, field of view phase = 178.8 mm, matrix size = 156 × 192, GRE read out TR = 6.2 ms, TE = 3 ms, number of averages = 1, shot TR = 10500 ms, shots per slice = 2, with one saturation pulse at a $\mathbf{B}_{1rms}$ of 3.06 μT with 500 ms duration. Raw CEST images were acquired at varying saturation offset frequencies from ±1.5 to ±4.5 ppm (relative to water resonance) with a step size of ±0.3 ppm. GRE images at two echo times (TE1 = 4.24 ms; TE2 = 5.26 ms) were collected to compute $\mathbf{B}_0$ map. $\mathbf{B}_1$ map was generated from the two images obtained using square preparation pulses with flip angles 30° and 60°. Overall, acquisition time of CEST images, $\mathbf{B}_1$ and $\mathbf{B}_0$ field maps is approximately 12 minutes. In brief, CEST images obtained from ±1.5 to ±4.5 ppm were interpolated using the cubic spline method to generate images with a fine step size of 0.01 ppm. $\mathbf{B}_0$ corrected CEST images at ±3 ppm were generated from the interpolated CEST images by picking signals according to the frequency shift in the $\mathbf{B}_0$ map. The $\mathbf{B}_0$ corrected ± 3.0 ppm images were then used for computing the percentage GluCEST contrast, which is equal to 100 x $(M_{-3ppm}-M_{+3ppm})/M_{-3ppm}$, where M_{-3ppm} and M_{+3ppm} are $\mathbf{B}_0$ corrected images saturated at -3ppm and +3ppm respectively with respect to water (7-9). $\mathbf{B}_1$ inhomogeneity artifacts in GluCEST maps were removed using $\mathbf{B}_1$ calibration curves as previously reported (10). The $\mathbf{B}_0$ and $\mathbf{B}_1$ corrected GluCEST contrasts were then averaged within expertly drawn regions-of-interest (ROIs). Finally, GluCEST values were extracted from the ROIs and quantified (Figure 2).

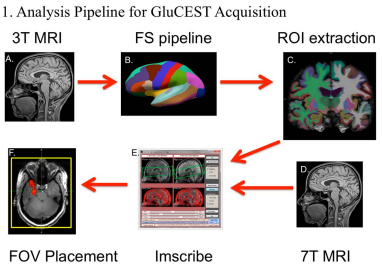

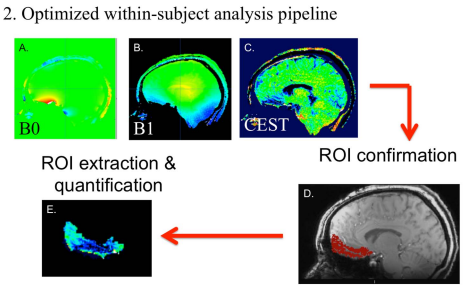

Results: GluCEST was 15% higher within the olfactory cortex ($p<.05$) in CR as compared to HC, but not within the medial orbitofrontal cortex (Figure C). Here, we not only demonstrate feasibility of imaging glutamate in primary olfactory cortex, but our results also suggest that GluCEST may be a useful marker in identifying those at risk for developing psychosis.

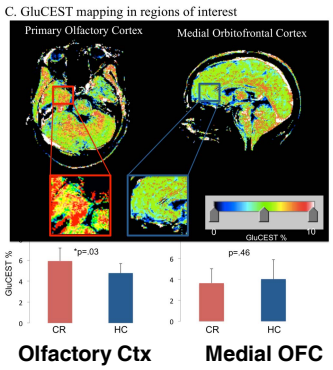

Conclusions: Our preliminary work indicates that youth at clinical risk for psychosis exhibit subtle, but significant abnormalities in GluCEST within the olfactory system. We suggest, that in addition to other metrics, neuroanatomical and neurochemical metrics of the olfactory system be considered as markers of risk. Moreover, our data indicates that high-resolution GluCEST MRI could help elucidate normal brain function and improve diagnosis of brain disorders associated with alterations in glutamate.

References: [1] Turetsky, B.I., et al., (2009) Schizophr Bull 35:1117-1131. [2] Kamath, V., (2011) Psychiatry Res 187:30-35. [3] Woodberry, K.A., Schizophr Res (2010) 123:188-198. [4] Brewer, W.J., Am J Psychiatry (2003) 160:1790-1794. [5] Maynard, T.M., et al., (2001) 27:457-476. [6] Wolf, D.H., et al., Psychopharmacology (2011) 218:503-512. [7] Cai, K., et al., Nat Med (2012) 18:302-306. [8] Haris, M., et al., NMR Biomed (2013) 26:386-391. [9] Crescenzi, R., et al., NeuroImage (2014) 101:185-192. [10] Singh, A., et al., Magn Reson Med (2013) 69:818-824.

Acknowledgements: R01MH099156 (BIT), K01MH102609 (DRR). This work is supported by the National Institute of Biomedical Imaging and Bioengineering under award number P41-EB015893, R01-NS087516.